

Effect of Electron Energy Sharing on the Double Photoionization of Helium Near Threshold

P. Lablanquie,¹ J. Mazeau,² L. Andric,² P. Selles,² and A. Huetz²

¹LURE, Batiment 209D, Université Paris Sud, 91405 Orsay, France

²Laboratoire de Dynamique Moléculaire et Atomique, CNRS et Université Pierre et Marie Curie, 4 Place Jussieu, T12-E5 75252 Paris Cedex 05, France

(Received 27 June 1994)

Energy and angle resolved measurements have been performed in the double photoionization of helium. Whereas the angular distributions do not depend much on the energy sharing (E_1, E_2) at 4 eV above threshold, a strong effect is observed at $E = 18.6$ eV. These results can be analyzed qualitatively if the total amplitude is split into two parts which are, respectively, symmetric (a_g) and antisymmetric (a_u) in the interchange of E_1 and E_2 , showing that the relative contribution of the latter increases with the excess energy. Dynamical effects of the energy on a_g are also noticeable in the measurements with equal sharing.

PACS numbers: 32.80.Fb

The double photoionization of a helium atom by a single photon offers the simplest situation for studying the correlations between two continuum electrons. This fundamental process is of main interest from the theoretical point of view, being a pure three-body problem on the atomic scale. A full treatment would involve the *ab initio* quantal calculation of an accurate six-dimensional wave function for the electron-ion-electron system, valid for short as well as long distances between the two electrons and the ion. Although such a goal is still out of reach, decisive progress has been accomplished recently and different approaches to obtaining the differential cross sections have been proposed [1,2].

On the experimental side complete information can be obtained if the two electrons are detected in coincidence after energy and angle selection, so that the triple-differential cross section (TDCS) is measured. Because of the extreme weakness of the latter, such measurements have become feasible only very recently [3–5]. If E_{ph} is the photon energy and $I = 79$ eV the double-ionization potential, then the two electrons share the excess energy above threshold: $E = E_{ph} - I = E_1 + E_2$. Most of the previous measurements were limited to the restricting case $E_1 = E_2 = E/2$ [3,4], where only one component of the ionization amplitude is involved (see below), but very recently a first experiment [5] at unequal sharing $E_1 \neq E_2$ was also performed far from threshold ($E = 52.9$ eV).

The aim of the present Letter is to report on experimental TDCS's that were obtained, for the first time, down to 4 eV above threshold and for energy sharing such as $E_1/E_2 = 0.2$ or 5, together with TDCS for equal sharing measured in the same conditions and at the same values of the total energy E . These measurements were performed using the highly polarized photon beam from the SU6 undulator line of Super Aco (Orsay, France), and the toroidal analyzer described in Ref. [4]. However, in contrast with the experiments reported in [4], only the second electron is detected here in the toroidal analyzer

for many angles simultaneously. The first electron flies through a tube which is placed inside the dead angle of the toroidal analyzer, and is detected by an additional 127° cylindrical analyzer, at right angles with respect to the photon beam. This arrangement allows one to make $E_1 = E_2$, as well as $E_1 \neq E_2$ measurements, in an extended angular range.

As shown in Ref. [4], the exact knowledge of the Stokes parameters associated with the photon beam is not important in the present geometry where the two electrons are detected in the $(\hat{k}, \hat{\varepsilon})$ plane defined by the beam direction \hat{k} and the main axis of polarization $\hat{\varepsilon}$. In the following measurements the energy resolutions are typically 500 meV in the cylindrical analyzer (E_1) and 300 meV in the toroidal analyzer (E_2). The angular acceptance out of the detection plane is $\pm 3^\circ$ for the two analyzers. In the detection plane the angular resolution is estimated to be 10° in the cylindrical analyzer (angle θ_1) and 20° in the toroidal analyzer (angle θ_2). Using the trigonometrical convention in the $(\hat{k}, \hat{\varepsilon})$ plane with the x axis along $\hat{\varepsilon}$, the angular range which is accessible for simultaneous measurements with the present apparatus is $30^\circ \leq \theta_2 \leq 330^\circ$, with two small forbidden regions along the photon beam ($80^\circ \leq \theta_2 \leq 100^\circ$ and $260^\circ \leq \theta_2 \leq 280^\circ$). On the other hand, a correct angular response of the apparatus relies on a good spatial uniformity of the electronic gain in the microchannel plate detector. Some points were discarded in the following figures, especially in the forward direction, when the latter criterion was not perfectly satisfied. Finally, the true coincidence count rate is higher than in the previous experiments [4], typically in the $10^{-2} - 10^{-1}$ Hz range and with a ratio of true to random coincidences between 1 and 10.

The TDCS measured at $E = 18.6$ eV above threshold are displayed on Fig. 1, for equal sharing [$E_1 = E_2 = 9.3$ eV, Fig. 1(a)] and unequal sharing [$E_1 = 15.6$ eV, $E_2 = 3$ eV, Fig. 1(b)] and $E_1 = 3$ eV, $E_2 = 15.6$ eV, Fig. 1(c)]. The first electron is detected along $\hat{\varepsilon}$ ($\theta_1 = 0$),

which implies that the mutual angle θ_{12} between the two electrons is given by $\theta_{12} = \theta_2 \pmod{\pi}$, $\theta_{12} \leq 180^\circ$. In these conditions the direction of $\hat{\epsilon}$ is an axis of symmetry [4]. Accordingly, the three figures appear to be almost symmetric with respect to $\hat{\epsilon}$, within the error bars. The results of Fig. 1(a) are consistent with those reported in [4] at neighboring energies ($E_1 = E_2 = 8.8$ eV). However, the present statistics are better, and the angular range is larger. Despite the finite energy and angular resolutions, the TDCS value is nearly zero at $\theta_{12} = 180^\circ$. In sharp contrast, this node is completely filled in Figs. 1(b) and 1(c), and becomes a clear maximum in the latter case. It is noticeable that the lobe observed when the higher-energy electron is fixed [Fig. 1(b)] is broader than in the reverse case [Fig. 1(c)].

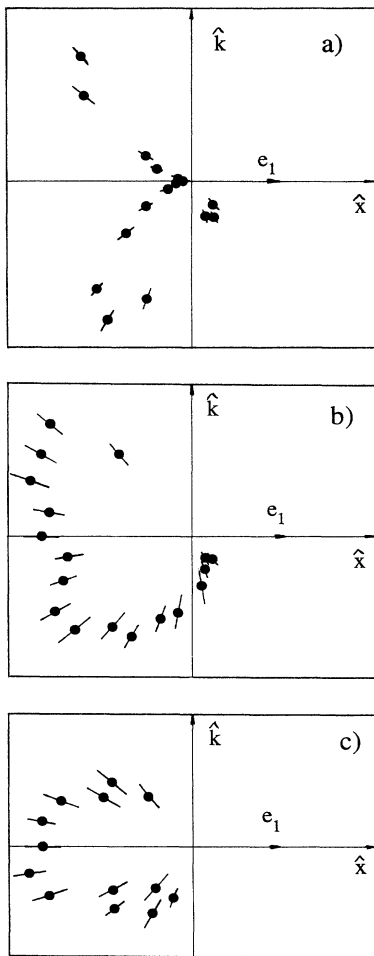


FIG. 1. Experimental TDCS at an excess energy $E = 18.6$ eV above threshold. The two electrons are detected in the $(\hat{k}, \hat{\epsilon})$ plane defined by the photon beam and by the direction of polarization. The x axis is taken along $\hat{\epsilon}$ and the first electron e_1 with energy E_1 is detected along x ($\theta_1 = 0$). The TDCS is plotted in polar coordinates with respect to the angle θ_2 locating the second electron with energy E_2 : (a) $E_1 = E_2 = 9.3$ eV; (b) $E_1 = 15.6$ eV and $E_2 = 3$ eV; and (c) $E_1 = 3$ eV and $E_2 = 15.6$ eV. The scales of (b) and (c) are identical (see text).

A completely opposite situation appears in Fig. 2, where similar measurements were performed at a much lower energy $E = 4$ eV. The data of Figs. 2(b) and 2(c) have slightly poorer statistics, due to the detection of a very low-energy electron (0.7 eV) that is more perturbed by stray electrons. However, the angular node at $\theta_{12} = 180^\circ$ exists in Figs. 2(a), 2(b), and 2(c), although it is slightly filled in Figs. 2(b) and 2(c). For equal sharing $E_1 = E_2 = 2$ eV, the value of the TDCS is zero at $\theta_{12} = 180^\circ$, within the error bars, and the two maxima which appear in Fig. 2(a) correspond to a mean value $\theta_{12} \approx 135^\circ$. For unequal sharing these maxima are still present at approximately the same angles, and the value of the TDCS at $\theta_{12} = 180^\circ$ can be estimated to be roughly 20% of the maxima. Apart from this tenuous filling at $\theta_{12} = 180^\circ$ there is no significant change observable between the Figs. 2(a), 2(b), and 2(c).

In order to analyze these dynamical effects of both the excess of energy above threshold and of its partitioning between the two electrons, it is convenient to recall the

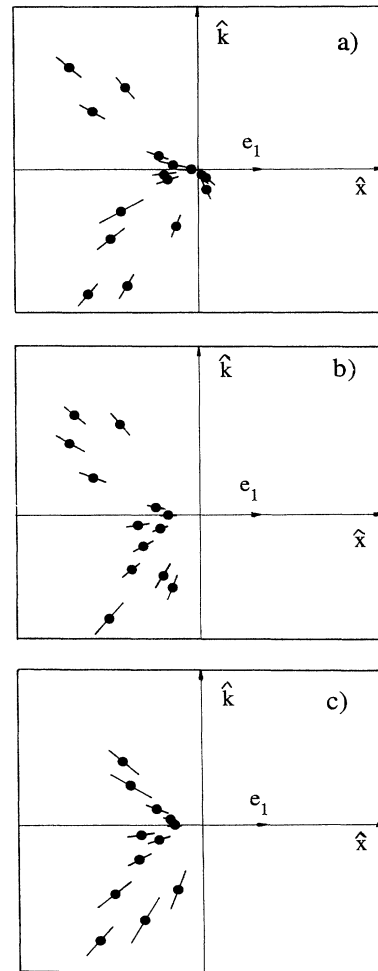


FIG. 2. Same as Fig. 1, but at $E = 4$ eV: (a) $E_1 = E_2 = 2$ eV; (b) $E_1 = 3.3$ eV and $E_2 = 0.7$ eV; and (c) $E_1 = 0.7$ eV and $E_2 = 3.3$ eV.

general expression that was established previously [4,6,7] for the TDCS in the present detection plane

$$\begin{aligned} \text{TDCS}(E_1, E_2) = & |a_g(E_1, E_2, \theta_{12}) (\cos\theta_1 + \cos\theta_2) \\ & + a_u(E_1, E_2, \theta_{12}) (\cos\theta_1 - \cos\theta_2)|^2. \end{aligned} \quad (1)$$

The two amplitudes a_g and a_u are unknown functions of E_1 , E_2 , and θ_{12} but they are, respectively, symmetric and antisymmetric in the interchange $E_1 \leftrightarrow E_2$: $a_g(E_1, E_2, \theta_{12}) = a_g(E_2, E_1, \theta_{12})$ and $a_u(E_1, E_2, \theta_{12}) = -a_u(E_2, E_1, \theta_{12})$. Expression (1) is fully general and exact, but dynamical models are needed to predict the dependence of both a_g and a_u amplitudes with respect to the energies E_1 and E_2 and to the mutual angle θ_{12} . On the other hand, valuable information on these amplitudes, i.e., on the dynamics, can be extracted directly from the present experiments, as we will now show.

In the conditions of Figs. 1 and 2 and when the second electron is emitted in the opposite direction ($\theta_{12} = 180^\circ$) expression (1) becomes

$$\text{TDCS}_{180^\circ}(E_1, E_2) = 4|a_u(E_1, E_2, 180^\circ)|^2. \quad (2)$$

In the special case of equal sharing ($E_1 = E_2 = E/2$) the antisymmetric amplitude a_u goes to zero for any θ_{12} and Eq. (2) implies a node in the cross section

$$\text{TDCS}_{180^\circ}(E/2, E/2) = 0.$$

Therefore, the antisymmetric amplitude $a_u(E_1, E_2, 180^\circ)$ is responsible at unequal sharing [Figs. 1(b), 1(c), 2(b), and 2(c)] for the filling of the node that exists at equal sharing [Figs. 1(a) and 2(a)]. Moreover, the TDCS in cases (a), (b), and (c) of Figs. 1 and 2 satisfy, respectively,

$$\text{TDCS}(E/2, E/2) = |a_g(E/2, E/2, \theta_{12})|^2(1 + \cos\theta_2)^2 = C(E, \theta_{12})(1 + \cos\theta_2)^2, \quad (3a)$$

$$\begin{aligned} \text{TDCS}(E_1, E_2) = & |a_g(E_1, E_2, \theta_{12})|^2(1 + \cos\theta_2)^2 + |a_u(E_1, E_2, \theta_{12})|^2(1 - \cos\theta_2)^2 \\ & + 2\text{Re}[a_g^*(E_1, E_2, \theta_{12})a_u(E_1, E_2, \theta_{12})](1 - \cos^2\theta_2), \end{aligned} \quad (3b)$$

$$\begin{aligned} \text{TDCS}(E_2, E_1) = & |a_g(E_1, E_2, \theta_{12})|^2(1 + \cos\theta_2)^2 + |a_u(E_1, E_2, \theta_{12})|^2(1 - \cos\theta_2)^2 \\ & - 2\text{Re}[a_g^*(E_1, E_2, \theta_{12})a_u(E_1, E_2, \theta_{12})](1 - \cos^2\theta_2), \end{aligned} \quad (3c)$$

with $E_1 + E_2 = E$ and $E_1 > E_2$.

At the lowest energy $E = 4$ eV, the general shapes in cases (b) and (c) are similar, as emphasized above. This implies that the cross terms in Eqs. (3b) and (3c) is small relative to the others, for any value of θ_{12} . Consequently, it is most probable that one of the two amplitudes is dominant in the whole angular range that was explored. Moreover, the latter is likely to be $a_g(E_1, E_2, \theta_{12})$ as a clear minimum at $\theta_{12} = 180^\circ$ exists in Figs. 2(b) and 2(c), which physically can only be due to the $(1 + \cos\theta_2)^2$ factor in Eqs. (3b) and (3c). Accordingly, the values of the TDCS at $\theta_{12} = 180^\circ$, given by Eq. (2), are small. Approximating the TDCS by its dominant term at $\theta_{12} = 140^\circ$, the ratio

$$|a_g(3.3, 0.7, 140^\circ)|/|a_u(3.3, 0.7, 180^\circ)| \approx 19$$

can be estimated from Figs. 2(b) and 2(c). Furthermore, if the contribution of the a_u amplitude is neglected, then the similarity of Fig. 2(a) with Figs. 2(b) and 2(c) proves that the θ_{12} dependence of the symmetric and dominant amplitude does not evolve significantly from equal to unequal sharing, at least up to E_1/E_2 or $E_2/E_1 = 5$.

A similar analysis of the results at $E = 18.6$ eV leads to drastically different conclusions. Equation (2) immediately leads to

$$\text{TDCS}_{180^\circ}(E_1, E_2) = \text{TDCS}_{180^\circ}(E_2, E_1),$$

and this relation gives a common scale for cases (b) and (c), which was used to plot Figs. 1(b) and 1(c). The difference that is observed between these two figures can

be attributed to the cross term of Eqs. (3b) and (3c). Subtracting the two curves point by point leads to two maxima of the latter, located symmetrically around $\theta_2 = 140^\circ$ and 220° and both corresponding to $\theta_{12} = 140^\circ$. The cross term being large the contributions of the two amplitudes must be comparable. The substantial value of the TDCS at 180° , which is a local measure of a_u , confirms that the latter is no longer negligible.

Finally, looking at Figs. 1(a) and 2(a) for equal sharing at $E = 18.6$ and 4 eV, respectively, some additional conclusions can be drawn. For angles θ_2 between 130° and 250° , corresponding to θ_{12} between 130° and 180° (left part of the figures), the analysis leads to values of $C(E, \theta_{12})$ [Eq. (3a)] comparable to those reported in Ref. [4], and no important change is observed between the two excess energies $E = 18.6$ and 4 eV. But lower values of θ_{12} , namely, 70° , 60° , and 50° were reached in the present measurements [right part of Figs. 1(a) and 2(a)]. The data show that in this region the TDCS decreases faster at the lower energy $E = 4$ eV than at the higher $E = 18.6$ eV. A rough estimate using Eq. (3a) and neglecting the effects of finite angular resolution leads to $C(18.6 \text{ eV}, \theta_{12} = 60^\circ) \approx 5 \times 10^{-3}$ and $C(4 \text{ eV}, \theta_{12} = 60^\circ) \approx 8 \times 10^{-4}$, if the two functions are normalized to 1 at $\theta_{12} = 180^\circ$, as in Ref. [4]. This strong energy dependence can be interpreted as a filter effect (see below).

In order to summarize all these observations it may be concluded that (i) the θ_{12} dependence of $a_g(E_1, E_2, \theta_{12})$

does not change significantly with E_1/E_2 at the lowest energy $E = 4$ eV; (ii) the amplitude $a_g(E_1, E_2, \theta_{12})$ depends critically on E for small values of θ_{12} , at least in the equal-sharing conditions $E_1 = E_2$ which are necessary to select it; (iii) the $a_u(E_1, E_2, \theta_{12})$ amplitude is almost negligible at the lowest energy $E = 4$ eV, with respect to a_g , but increases with E to a comparable influence on the TDCS around $E = 18.6$ eV. It is worthwhile here to discuss these conclusions in the light of available theories. Obviously the unequal sharing situation is the most severe test, as it involves the two a_g and a_u amplitudes and interference effects between them. Calculations based on a so-called 3C wave function for the final state [1] have proved to reproduce the shape of the TDCS for equal sharing at $E = 20$ and 10 eV remarkably well [1,3]. For unequal sharing the same theory also agrees well with the recent experiment [5] performed at $E = 52.9$ eV. However, at lower energy ($E = 1$ eV) these calculations [1] in the velocity form exhibit a dependence on the $E_1 \leftrightarrow E_2$ interchange, and give a maximum of the TDCS at $\theta_{12} = 180^\circ$ ($E = 1$ and 5 eV). This is not consistent with the present observations at $E = 4$ eV and requires further investigation. On the other hand, at low energy a prediction was formulated [8] based on the threshold theory of Wannier [9]. It was shown that $|a_u|^2$ and $|a_g|^2$, which correspond to the two components of the final state with, respectively, zero and nonzero densities on the Wannier ridge, should follow different threshold laws. Taking into account a subsequent correction [10], these threshold laws are

$$|a_g|^2 \propto E^{m-2}, \quad |a_u|^2 \propto E^{3m-3/2},$$

with $m = 1.056$ for double photoionization. Note that integration over angles and E_1 leads, respectively, to the two exponents 1.056 and 3.17 at the level of integral cross sections [6]. When E decreases towards zero, $|a_u|^2$ becomes necessarily smaller than $|a_g|^2$, and the "threshold region" can be defined as the region where $|a_g|^2$ dominates. This is fully consistent with the above observation (iii) of a small $|a_u|^2$ at $E = 4$ eV, but with such criteria this energy appears to be slightly out of the threshold region, as some effects due to a_u can be observed. This also agrees with previous measurements of the integral cross section [11] showing that the $E^{1.056}$ threshold law only applies up to 2 eV. On the other hand, the manifestation of the a_u amplitude at $E = 18.6$ eV implies that the threshold regime can no longer apply at such energy. A rapid look at the results of Ref. [5] seems to indicate that this growing influence of a_u continues at higher energy.

The simplifying hypotheses which were made at first [12] to predict the angular correlation from the dynamical model of Wannier can be removed and more accurate calculations performed, at least in the case of equal shar-

ing [2]. Using the picture developed in this model, the initial state distribution with respect to θ_{12} is transformed when propagated through the Coulomb region. The latter plays the role of a filter which attenuates the distribution especially for values of θ_{12} far from $\theta_{12} = 180^\circ$, which is a stable point with respect to Coulomb forces. The above observation (ii) confirms this picture and proves that from $E = 18.6$ down to $E = 4$ eV the more spectacular effects occur in the wing of the angular distribution ($\theta_{12} = 60^\circ$) which is more and more "filtered" when E decreases. However, a decrease of the width of $C(E, \theta_{12})$ with E is expected in the threshold region below 4 eV, and this will be the object of future experiments.

In conclusion, the present results give some preliminary insight into the detailed dynamics of the double photoionization of helium, for energies ranging from threshold up to 20 eV above. Equation (1) provides a general frame for analysis, as it includes all symmetry and angular properties, and allows us to isolate the dynamical effects. It is clear, however, that more extensive and accurate measurements of the same type will be necessary to complete the knowledge of this fundamental three-body process.

We are most grateful to the staff of Super-ACO and LURE for providing us with excellent facilities and assistance during the course of this work.

-
- [1] F. Maulbetsch and J.S. Briggs, *J. Phys. B* **26**, L647 (1993); **26**, 1679 (1993); **27**, 4095 (1994).
 - [2] A.K. Kazansky and V.N. Ostrovsky, *J. Phys. B* **27**, 443 (1994); *J. Phys. IV (France)* **6**, 159 (1993).
 - [3] O. Schwarzkopf, B. Krässig, J. Elmiger, and V. Schmidt, *Phys. Rev. Lett.* **70**, 3008 (1993); O. Schwarzkopf, B. Krässig, and V. Schmidt, *J. Phys. IV (France)* **6**, 169 (1993).
 - [4] A. Huetz, P. Lablanquie, L. Andric, P. Selles, and J. Mazeau, *J. Phys. B (France)* **27**, L13 (1994).
 - [5] O. Schwarzkopf, B. Krässig, V. Schmidt, F. Maulbetsch, and J.S. Briggs, *J. Phys. B* **27**, L347 (1994).
 - [6] A. Huetz, P. Selles, D. Waymel, and J. Mazeau, *J. Phys. B* **24**, 1917 (1991).
 - [7] D. Waymel, L. Andric, J. Mazeau, P. Selles, and A. Huetz, *J. Phys. B* **26**, L123 (1993).
 - [8] C.H. Greene and A.R.P. Rau, *Phys. Rev. Lett.* **48**, 533 (1982); *J. Phys. B* **16**, 99 (1983).
 - [9] G.H. Wannier, *Phys. Rev.* **90**, 817 (1953).
 - [10] R. Peterkop, *J. Phys. B* **16**, L587 (1983).
 - [11] H. Kossmann, V. Schmidt, and T. Andresen, *Phys. Rev. Lett.* **60**, 1266 (1988).
 - [12] A.R.P. Rau, *J. Phys. B* **9**, L283 (1976); J.M. Feagin, *J. Phys. B* **17**, 2433 (1984); D.S.F. Crothers, *J. Phys. B* **19**, 463 (1986).